# Neutral and Cationic Heteroscorpionate Aluminum Complexes: Synthesis, Structure, and Ring-Opening Polymerization of ϵ-Caprolactone

Stefano Milione,*,† Fabia Grisi,† Roberto Centore,‡ and Angela Tuzi‡

*Dipartimento di Chimica, Università di Salerno, 84081 Baronissi, Italy, and Dipartimento di Chimica, Università di Napoli "Federico II", Complesso Universitario di Monte S. Angelo, Via Cinthia, 80126 Napoli, Italy*

*Received October 18, 2005*

Treatment of 2,4-di-*tert*-butyl-6-(bis(3,5-dimethylpyrazol-1-yl)methyl)phenol (*bpzmp*-H) as tridentate ligand with aluminum trialkyls affords the corresponding heteroscorpionate aluminum complexes (*bpzmp*)-$AlR_2$ (R = Me (**1**); R = Et (**2**); R = *i*Bu (**3**)) in high yield. In the solid state, complexes **1**−**3** were isolated as racemic mixtures in which each stereoisomer adopts a tetrahedral structure with the *bpzmp* ligand $\kappa^2$-coordinated to the metal via the phenoxy group and the imino nitrogen of one of pyrazolyl rings. The investigation of the solution structure of **1**−**3** by means of VT $^1$H NMR spectroscopy revealed fluxional exchange between coordinated and noncoordinated pyrazolyl rings, producing interconversion between the two enantiomers. The activation enthalpy ($\Delta H^{\#}$) for racemization processes (10.1 ± 0.2 kcal·mol$^{-1}$ (**1**); 11.6 ±0.3 kcal·mol$^{-1}$ (**2**); 14.1 ± 0.2 kcal·mol$^{-1}$ (**3**)) was dependent on steric hindrance at the aluminum center. Reaction of **1** or **2** with $B(C_6F_5)_3$ proceeds through net alkyl abstraction, forming the expected cationic aluminum complexes $[(bpzmp)AlR]^+[RB(C_6F_5)_3]^-$ (R = Me (**4**); R = Et (**5**)), in which the *bpzmp* fragment acts as a tridentate ligand. The ionization reaction of **3** with Lewis acidic compounds ($B(C_6F_5)_3$ or $[Ph_3C][B(C_6F_5)_4]$) proceeds by net $\beta$-H abstraction from the isobutyl group, forming $[(bpzmp)Ali\text{Bu}]^+[HB(C_6F_5)_3]^-$ (**6**) along with isobutene; in contrast, reaction with the Brönsted acid $[HNMe_2Ph][B(C_6F_5)_4]$ proceeds by protonolysis of the isobutyl group. Complex **4** is active in ring-opening polymerization of ϵ-caprolactone (ϵ-CL), producing high-molecular-weight polymers. The $^1$H NMR monitoring of the reaction between **4** and ϵ-CL in 1:1 molar ratio showed that the initiation involves monomer insertion into the Al−O bond of the *bpzmp* fragment, forming the intermediate $[(bpzphe)AlMe]^+[MeB(C_6F_5)_4]^-$ (*bpzphe* = 2,4-di-*tert*-butyl-6-(bis(3,5-dimethylpyrazol-1-yl)methyl)phenyl 6-hydroxyhexanoate (**8**). The growth of the polymer chain occurs through continuous insertions of the monomer in the Al−alkoxide bond.

## Introduction

In recent years there has been a growing interest in the synthesis of cationic aluminum complexes because the enhanced Lewis acidity of the aluminum center should yield greater catalytic activity and may lead to new applications.[1] Some cationic complexes have already found application in ethylene,[2] alkene oxide,[3] and D,L-lactide[4] polymerization catalysis.

In this context tri- and tetracoordinate cationic aluminum alkyls are particularly attractive, because they combine cationic charge and low coordination number, producing an increased electrophilic character at the metal. Such cationic species can be generated by reaction of aluminum dialkyl precursors, bearing monoanionic bidentate ($LX^-$) or tridentate ($L_2X^-$) ligands, with $[Ph_3C][B(C_6F_5)_4]$ or $B(C_6F_5)_3$ via alkyl abstraction at the metal center[2c,d] or with ammonium salts $[HNR_3][B(C_6F_5)_4]$ via alkane elimination, affording stable amine adducts.[5] While ionization of neutral aluminum dialkyls $(L_2X)AlR_2$ usually generates stable four-coordinate cationic aluminum species,[2d,6] that of $(LX)AlR_2$ complexes may yield more reactive tricoordinate aluminum alkyl cations due to the absence of a second ligand for stabilizing the cationic aluminum center.[7]

Several studies have shown that the stability of these cationic species is strongly dependent on the inertness of the counterion and on the presence of a Lewis base $L^1$ that can stabilize the aluminum cation by forming $\{LX\}Al(R)(L^1)^+$ adducts.[8] Gibson

* To whom correspondence should be addressed. E-mail: smilione@unisa.it.

† Università di Salerno.

‡ Università di Napoli "Federico II".

(1) (a) Atwood, D. A. *Coord. Chem. Rev.* **1998**, *176*, 407. (b) Atwood, D. A.; Yearwood, B. C. *J. Organomet. Chem.* **2000**, *600*, 186−197.

(2) For leading references, see: (a) Bochmann, M.; Dawson, D. M. *Angew. Chem., Int. Ed. Engl.* **1996**, *35*, 2226. (b) Coles, M. P.; Jordan, R. F. *J. Am. Chem. Soc.* **1997**, *119*, 8125. (c) Bruce, M.; Gibson, V. C.; Redshaw, C.; Solan, G. A.; White, A. J. P.; Williams, D. J. *Chem. Commun.* **1998**, 2523. (d) Kim, K.-C.; Reed, C. A.; Long, G. S.; Sen, A. *J. Am. Chem. Soc.* **2002**, *124*, 7662.

(3) (a) Atwood, D. A.; Jegier, J. A.; Rutherford, D. *J. Am. Chem. Soc.* **1995**, *117*, 6779. (b) Jegier, J. A.; Atwood, D. A. *Inorg. Chem.* **1997**, *36*, 2034. (c) Munoz-Hernandez, M.-A.; Sannigrahi, B.; Atwood, D. A. *J. Am. Chem. Soc.* **1999**, *121*, 6747.

(4) Emig, N.; Nguyen, H.; Krautscheid, H.; Reau, R.; Cazaux, J.-B.; Bertrand, G. *Organometallics* **1998**, *17*, 3599.

(5) Korolev, A. V.; Ihara, E.; Guzei, I. A.; Young, V. G., Jr.; Jordan, R. F. *J. Am. Chem. Soc.* **2001**, *123*, 8291.

(6) (a) Cameron, P.; Gibson, V. C.; Redshaw, C.; Segal, J. A.; Bruce, M. D.; White, A. J. P.; Williams, D. J. *Chem. Commun.* **1999**, 1883. (b) Cameron, P.; Gibson, V. C.; Redshaw, C.; Segal, J. A.; Bruce, M. D.; White, A. J. P.; Williams, D. J. *J. Chem. Soc., Dalton Trans.* **2002**, 415.

(7) (a) Ihara, E.; Young, V. G., Jr.; Jordan, R. F. *J. Am. Chem. Soc.* **1998**, *120*, 8277. (b) Radzewich, C. E.; Guzei, I. A.; Jordan, R. F. *J. Am. Chem. Soc.* **1999**, *121*, 8673. (c) Dagorne, S.; Lavanant, L.; Welter, R.; Chassenieux, C.; Haquette, P.; Jaouen, G. *Organometallics* **2003**, *22*, 3732.

10.1021/om050902e CCC: $33.50 
Publication on Web 11/23/2005

**Chart 1**

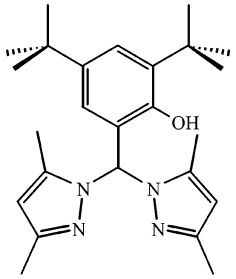


bpzmp-H

et al. showed that a pendant donor group that in the neutral aluminum complexes is weakly bonding or nonbonding became a normal donor group in the cationic derivatives upon reaction with $B(C_6F_5)_3$, thus stabilizing these species. Corresponding cations could not form in the absence of these additional donors.[6b] Bertrand et al. reported the use of anionic tridentate nitrogen ligands to obtain neutral and cationic tetracoordinate aluminum complexes.[9] In all cases, these tridentate nitrogen donors enforce an approximately trigonal-monopyramidal coordination geometry through the formation of a rather rigid bicyclic core. As a result of this unusual geometry, the empty axial coordination site is accessible for substrate binding. Preliminary results have shown that these metal-based Lewis acids are promising catalysts for ring-opening polymerization of heterocycles.

To expand this class of compounds, we were interested in the tridentate heteroscorpionate ligand 2,4-di-*tert*-butyl-6-(bis-(3,5-dimethylpyrazol-1-yl)methyl)phenol (*bpzmp*-H) (Chart 1). Heteroscorpionates represent one of the most versatile types of tridentate ligands that can coordinate to a wide variety of elements, e.g., from early to late transition metals, and the coordination chemistry of these systems has developed greatly in recent years.[10] Up to now no reports on coordination chemistry of this heteroscorpionate ligand with a main group metal exist in the scientific literature.

Here, the application of this ligand toward the synthesis of neutral and cationic aluminum alkyl complexes is reported, including the structural characterization of the heteroscorpionate aluminum complexes. Their dynamic behavior in solution is discussed, and their reactivity toward ring-opening polymerization of $\epsilon$-caprolactone is reported.

## Results and Discussion

**1. Synthesis and Structure of Neutral Complexes (*bpzmp*)-$AlR_2$ (R = Me (1), R = Et (2), R = *t*Bu (3)).** 2,4-Di-*tert*-butyl-6-(bis(3,5-dimethylpyrazol-1-yl)methyl)phenol (*bpzmp*-H) as tridentate ligand readily reacts with 1 equiv of $AlMe_3$, $AlEt_3$, or Al-*i*$Bu_3$ to form monomeric (*bpzmp*)$AlR_2$ (R = Me (**1**), R = Et (**2**), R = *i*Bu (**3**)), with elimination of the corresponding alkane (Scheme 1). These reactions proceed readily in hydrocarbon solvents (e.g., hexane, toluene) at room temperature, resulting in nearly quantitative conversion to the dialkyl species. **1**, **2**, and **3** are very soluble in hydrocarbon solvents, and single crystals were obtained by recrystallization from saturated solutions at low temperature.

**Scheme 1**

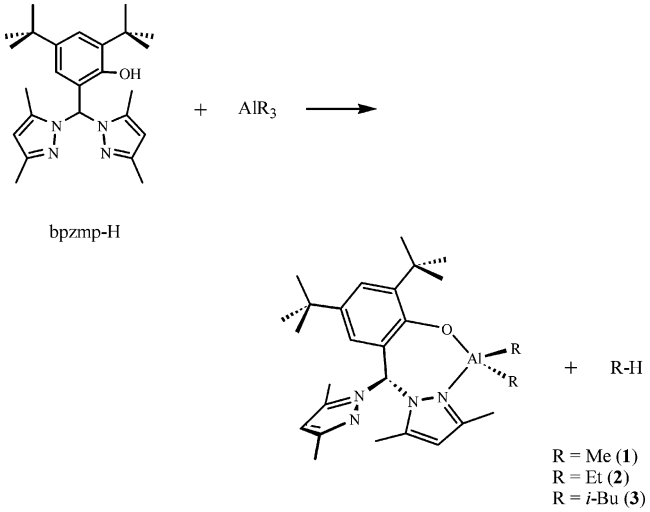


Molecular structures of **1**−**3** were determined by X-ray analysis (Figure 1). In all the cases, the heteroscorpionate ligand is $\kappa^2$-N,O$^-$ coordinated to Al, forming tetrahedral complexes with $C_1$ symmetry. While some cases of N,N-bidentate coordination are already reported,[10c] this kind of coordination was never observed before.

The geometry around Al can be described for all complexes as tetrahedral distorted; in fact, the dihedral angle between N2−Al−O1 and C−Al−C planes (87.9(2)°, 89.3(2)°, and 89.91(7)° for **1**, **2**, and **3**) is in agreement with tetrahedral geometry, but angles at Al show considerable deviation from ideal values (range 98.2(2)° to 115.6(2)° for **1**, 102.0(2)° to 120.1(3)° for **2**, 103.62(7)° to 116.6(1)° for **3**). In all cases the most acute angle is observed for N2−Al−O1, which is constrained by the bite of the bischelate ligand in a seven-membered ring. Within the coordination sphere of Al, the bond distance Al−O1 (1.753(4), 1.738(2), 1.771(2) Å for **1**, **2**, and **3**) is shorter than Al−N2 (1.976(5), 1.961(3), 2.009(2) Å for **1**, **2**, and **3**) and Al−C distances (mean value 1.967, 1.973, and 1.974 Å for **1**, **2**, and **3**, respectively), and values found are in good agreement with literature data.[5b] This effect is probably

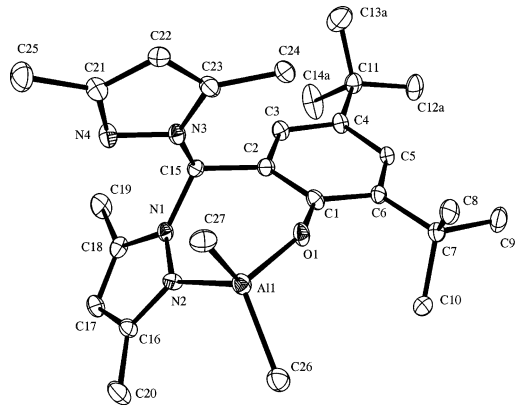


**Figure 1.** ORTEP view of **1**. Thermal ellipsoids at the 30% probability level; H atoms, toluene solvent molecule, and one of the statistical *tert*-butyl groups are not shown for clarity. Selected bond distances (Å): Al−N2 1.968(4), Al−O1 1.748(3), Al−C26 1.973(5), Al−C27 1.962(5), N1−N2 1.378(5), O1−C1 1.338(5). Selected bond angles (deg): O1−Al−C26 108.8(2), C26−Al−C27 115.6(2), O1−Al−N2 98.2(2), C27−Al−N2 109.1(2), C26−Al−N2 109.9(2), C1−O1−Al 48.2(3). Selected torsion angles (deg): C2−C15−N1−N2 75.4(5), N1−C15−C2−C1 −62.4(5), N2−Al−O1−C1 2.8(6), O1−Al−N2−N1 −28.8(3).

(8) Dagorne, S.; Guzei, I. A.; Coles, M. P.; Jordan, R. F. *J. Am. Chem. Soc.* **2000**, *122*, 274.

(9) Emig, N.; Nguyen, H.; Krautscheid, H.; Reau, R.; Cazaux, L. B.; Bertrand, G. *Organometallics* **1998**, *17*, 3599.

(10) Otero, A.; Fernandez-Baeza, J.; Antinolo, A.; Tejeda, J.; Lara-Sanchez, A. *Dalton Trans.* **2004**, 1499.

**Scheme 2**

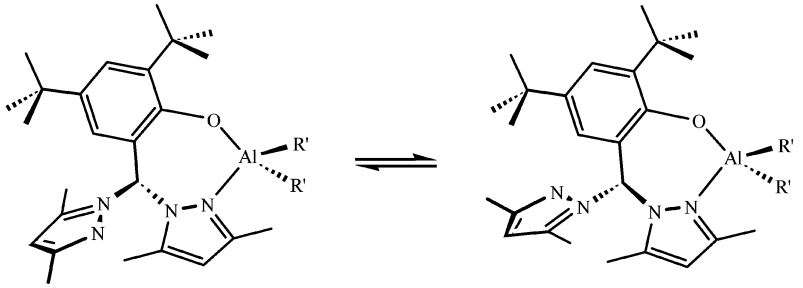

R' = Me (**1**), Et (**2**), *i*Bu (**3**).

due to significant $\pi$ contributions to the Al−O bond from lone pairs of O atoms.[11] The alkyl groups bound to Al seem to have a relatively high degree of conformational freedom, by rotation around Al−C and C−C bonds; in fact, a statistical positional disorder is found for these groups in **2** and **3**.

It is worth noting that, given the coordination mode of heteroscorpionate ligands, complexes **1**−**3** are chiral compounds. They crystallize as a racemic mixture with both enantiomers included in the unit cells belonging to centrosymmetric space groups.

Compounds **1**−**3** do not further react with the heteroscorpionate ligand to give bis-adduct derivatives. Treatment of a benzene solution of **1**−**3** in a NMR tube with 1 equiv of *bpzmp*-H at room temperature produces no change in the proton spectra, also after several hours. A similar behavior was already observed for the three-benzyl heteroscorpionate zirconium complex, and it was attributed to the relative bulkiness of the ligand and complex.[12]

**2. Dynamic Behavior of Solution Structures of 1−3.** The $^1$H NMR spectrum of **1** at room temperature is not consistent with its crystal structure. The number of $^1$H signals indicates the presence of a highly symmetric structure; in fact only one set of resonances is observed for the two nonequivalent pyrazolyl rings. Moreover the signals of the methyl groups at the aluminum center appear as a unique broad resonance at 0.54 ppm. The VT NMR analysis shows that at subambient temperature the resonances of methyl groups bound to aluminum as well as those of pyrazolyl rings and the resonance of the H$^4$ of the same rings broaden and resolve each in two separate peaks. At −60 °C the resonances become sharp and well resolved and the NMR spectrum becomes consistent with the observed solid-state structure. This picture indicates the presence of an exchange process between the coordinated and the noncoordinated pyrazolyl rings, resulting in the interconversion from one stereoisomer to the other (Scheme 2). At ambient temperature the exchange is fast, on the NMR time scale, and so the two pyrazolyl rings appear equivalent. The rate constants at different temperature are evaluated by comparison of experimental with simulated spectra obtained using a full line shape calculation program.[13] At 20 °C the rate constant is 2840 $s^{-1}$ and the activation free energy is 7.7 ± 0.1 kcal·mol$^{-1}$. The enthalpy ($\Delta H^{\#}$) and the entropy of activation ($\Delta S^{\#}$) are evaluated from the Eyring plot, and values are 10.1 ± 0.2 kcal·mol$^{-1}$ and 8.0 ± 0.8 cal mol$^{-1}$ K$^{-1}$, respectively.

The same fluxional behavior was observed for **2** and **3** but with higher activation barriers. At ambient temperature **2** is close to the coalescence point (293 K), while **3** is in the region of slow exchange. The rate constants ($k$) at room temperature are 326 and 2 $s^{-1}$ for **2** and **3**, respectively. The small value of $k$ for racemization of **3** makes its $^1$H NMR spectrum consistent with the solid-state structure (at room temperature). The activation parameters were determined by VT NMR analysis, and the corresponding values are reported in Table 1.

**Table 1. Summary of Kinetic Parameters for Racemization of (*bpzmp*)AlMe$_2$ (1), (*bpzmp*)AlEt$_2$ (2), and (*bpzmp*)Ali*Bu$_2$ (3)**

| | $k$ (at 293 K), $s^{-1}$ | $\Delta G^{\#}$ (at 293 K), kcal·mol$^{-1}$ | $\Delta H^{\#}$, kcal·mol$^{-1}$ | $\Delta S^{\#}$, cal·mol$^{-1}$·K$^{-1}$ |
|---|---|---|---|---|
| **1** | 2840 | 7.7 ± 0.1 | 10.1 ± 0.2 | 8.0 ± 0.8 |
| **2** | 326 | 9.5 ± 0.1 | 11.6 ± 0.3 | 7.3 ± 0.9 |
| **3** | 2 | 11.4 ± 0.1 | 14.1 ± 0.2 | 9.1 ± 0.6 |

Two different mechanisms for the racemization of **1**−**3** can be drawn. The first is a displacement mechanism ($S_N2$) in which the pyrazolyl ring that is out of the coordination sphere of Al displaces the pyrazolyl ring coordinated at Al in a one-step reaction. The approach of the free pyrazolyl ring is necessarily from the opposite side of the coordinated pyrazolyl ring so inversion of configuration at Al center occurs. The second pathway is a dissociation mechanism that proceeds by a two-step reaction ($S_N1$). In the first step the pyrazolyl ring coordinated at Al goes out from the coordination sphere of Al, producing a three-coordinate Al complex; in the second step, one of the two free pyrazolyl rings coordinates to Al, forming the four-coordinate complex. In this step both stereoisomers can be formed. To distinguish between these two mechanisms, the activation parameters are analyzed as a function of the steric hindrance at the aluminum center (Table 1). The increase of the enthalpy of activation with increasing steric hindrance on the aluminum and the substantial invariance of the entropy of activation with the bulkiness of the substituents support the $S_N2$ mechanism.

It is worth noting that a similar exchange of coordinated and uncoordinated pyrazolyl groups was already observed in tris(pyrazolyl)hydroborato aluminum complexes {$\eta^2$-HB(3-*t*Bupz)$_3$}-AlMe$_2$[14] and {H(3-*t*Bupz)B(3-*t*Bupz)(5-*t*Bupz)-$\eta^2$}AlEt$_2$.[14] By inspection of NMR data Chisholm and al.[15] similarly concluded that the dynamic exchange process involves an intramolecular associative displacement of one pz group for the other.

The $^{27}$Al NMR spectrum for **1**−**3** was also recorded; for all the samples, a broad resonance was recorded in the region expected for a four-coordinate aluminum center,[16] apart from alkyl substituents on aluminum.

(11) Barron, A. R.; Dobbs, K. D.; Francl, M. M. *J. Am. Chem. Soc.* **1991**, *113*, 39.

(12) Milione, S.; Montefusco, C.; Grassi, A.; Cuenca, T. *Chem Commun.* **2003**, 1176.

(13) *WINDNMR* (DNMR71.EXE) is a window program for simulating high-resolution NMR spectra.

(14) Looney, A.; Parkin, G. *Polyhedron* **1990**, *9*, 265.

(15) Chisholm, M. H.; Eilerts, N. W.; Huffman, J. C. *Inorg. Chem.* **1996**, *35* (2), 445.

(16) (a) Atwood, D. A.; Harvey, M. *J. Chem. Rev.* **2001**, *101*, 37. (b) Zhang, Z.; Dijkstra, R. J.; Feijen, J. *Angew. Chem., Int. Ed.* **2002**, *41*, 4510. (c) Benn, R.; Rufinska, A. *Angew. Chem., Int. Ed. Engl.* **1986**, *25*, 861.

**Scheme 3**

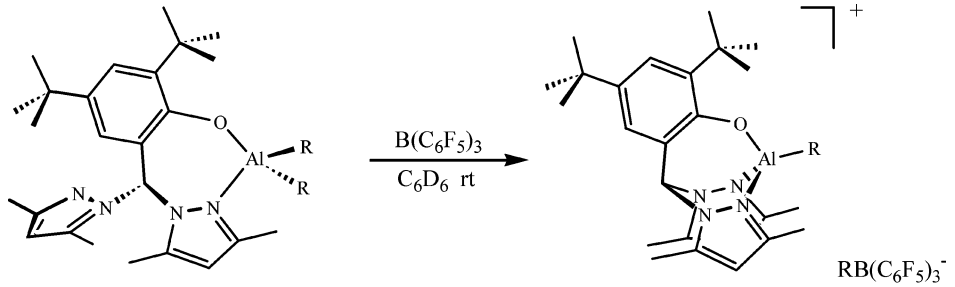


R = Me (**4**), Et (**5**)

**3. Synthesis and Characterization of Cationic Complexes [(*bpzmp*)AlR$^1$]$^+$[R$^2$B(C$_6$F$_5$)$_3$]$^-$ (R$^1$ = R$^2$ = Me (4); R$^1$ = R$^2$ = Et (5); R$^1$ = *i*Bu, R$^2$ = H (6); R$^1$ = *i*Bu, R$^2$ = C$_6$F$_5$ (7)).** The generation of cationic derivatives of the heteroscorpionate alkyl aluminum complexes has been explored by reacting the neutral aluminum complexes with an alkyl-abstracting agent. $B(C_6F_5)_3$ has been used successfully to generate reactive metal $LnAlR^+$ cations from $LnAlR_2$ precursors.[2,17] However, the resulting $RB(C_6F_5)_3^-$ anions are often incompatible with $LnAlR^+$ species due to $R^-$ or $C_6F_5^-$ transfer leading to neutral products.[18]

Treatment of **1** with 1 equiv of $B(C_6F_5)_3$ affords the expected cationic monomethyl species (*bpzmp*)AlMe$^+$ (**4**) as a borate salt (Scheme 3) in good yield (70%). $^1$H NMR monitoring of the reaction in a NMR tube showed that this is fast and quantitative in a few minutes. Complex **4** is very soluble in halogenated and aromatic solvents, but on standing, it slowly decomposes to unknown species, hampering the crystallization.[19] In a crystallization attempt from $CH_2Cl_2$/hexane, the salt [3,5-Me$_2$-$C_3H_3N_2$]$^+$[MeB(C$_6$F$_5$)$_3$]$^-$ (**4a**) was recovered, and its X-ray structure is reported in Figure 2.

The molecular structure of **4** was defined in solution by NMR spectroscopy. In the $^1$H NMR spectrum of **4** the methyl group bound at the aluminum center appears as a sharp singlet at −0.12 ppm, and the resonances for the *bpzmp* fragment were high field shifted with respect to the neutral complex (observed in the range of fast exchange). The two pyrazolyl rings appear equivalent, indicating the presence of a mirror plane passing through the molecule. We suggest that in this case both pyrazolyl rings coordinate the cationic center, forming a tetracoordinate alkyl aluminum cation in which the ligand is in "*s-cis*" conformation and $\kappa^3$-N,N,O-coordinated to the metal center. A similar stabilizing effect by a pendant arm was already observed by Gibson et al.; they found that a weakly bonding or nonbonding donor arm in the neutral precursor becomes a strong ligand occupying the fourth coordination position in the cation, thereby stabilizing the electropositive aluminum center.[5b]

The methyl group of [MeB(C$_6$F$_5$)$_3$]$^-$ in the $^1$H NMR spectrum of **4** appeared at 0.96 ppm, indicating that the anion is substantially not coordinated to the aluminum cation. As matter of fact, tight ion pairs with methyl bridges show signals at ca. $\delta$ 0.1, as in Cp$^2$ZrMe($\mu$-Me) B(C$_6$F$_5$)$_3$,[20] whereas the free anion shows chemical shifts around $\delta$ 1.3. The noncoordinating nature of the [MeB(C$_6$F$_5$)$_3$]$^-$ anion is further confirmed by the small chemical shift difference ($\Delta\delta$ 2.6 ppm) between the *m*- and *p*-fluorine $^{19}$F NMR resonances.[21]

Similarly, treatment of **2** with 1 equiv of $B(C_6F_5)_3$ clearly affords the cationic monoethyl complex [(*bpzmp*)AlEt]$^+$ [EtB(C$_6$F$_5$)$_3$]$^-$ (**5**) in quantitative yield (Scheme 3). In the $^1$H NMR spectrum of complex **5** the same pattern of resonances for the coordinated ligand as in **4** is observed. So $\kappa^3$ coordination of the ligand is also proposed for **5**. The ethyl group bound at the aluminum center in **5** gives rise to an $A_2X_3$ system and appears as a quartet and a triplet centered at 0.47 and 1.36 ppm, respectively. The [EtB(C$_6$F$_5$)$_3$]$^-$ anion has characteristic resonances at 1.72 ppm (vbr q) and 1.08 ppm (t, $J$ = 6.8 Hz); also in this case the small chemical shift difference between the *o*-F and *p*-F $^{19}$F NMR resonances ($\Delta\delta$ 2.6 ppm) indicates a noncoordinative character.[21]

It is worth noting that proton resonances for both cationic derivatives **4** and **5** are sharp and well resolved, indicating elevated coordination energy of the ligand to the metal center and the absence of any fluxional equilibrium involving the neutral moiety of the ligand.

The reactions between **1** or **2** and $B(C_6F_5)_3$ proceeds by net alkyl abstraction from aluminum compounds as expected, while reaction of the isobutyl derivative **3** with $B(C_6F_5)_3$ occurs by net $\beta$-H abstraction, giving [(*bpzmp*)Al*i*Bu]$^+$[HB(C$_6$F$_5$)$_3$]$^-$ (**6**), together with 1 equiv of isobutene (Scheme 4). The reaction is fast and quantitative on the NMR scale. Complex **6** shows the same $C_s$ symmetry observed for the homologous cations with a strong $\kappa^3$-N,N,O coordination of the ligand. The isobutyl group

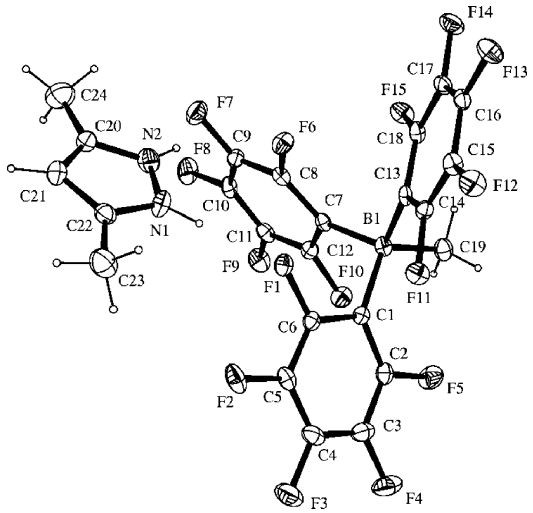


**Figure 2.** ORTEP view of **4a**. Thermal ellipsoids at the 30% probability level. Selected bond distances (Å): B1−C19 1.626(5), N1−N2 1.339(4), N1−C22 1.327(4).

(17) For other reports of ethylene polymerization by Al catalysts see: (a) Kim, J. S.; Wojcinski, L. M.; Liu, S.; Sworen, J. C.; Sen, A. *J. Am. Chem. Soc.* **2000**, *122*, 5668. (b) Soga, K.; Shiono, T.; Doi, Y. *J. Chem. Soc., Chem. Commun.* **1984**, 840. (c) Martin, H.; Bretinger, H. *Makromol. Chem.* **1992**, *193*, 1283.

(18) (a) Qian, B.; Ward, D. L.; Smith, M. R., III. *Organometallics* **1998**, *17*, 3070. (b) Deckers, P. J. W.; Van der Linden, A. J.; Meetsma, A.; Hessen, B. *Eur. J. Inorg. Chem.* **2000**, 929.

(19) Monitoring a $C_6D_6$ solution of **4** showed that the concentration of **4** decreased by 16% after a week at 50 °C.

**Scheme 4**

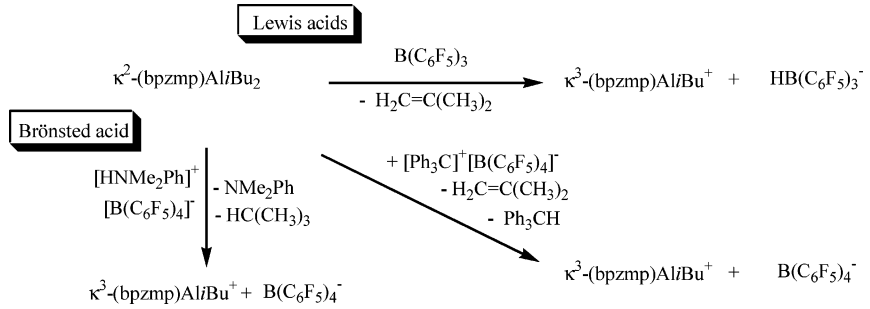


in **6** appears as an $A_2MX_6$ system with a multiplet centered at 2.28 and two doublets centered at 1.23 and 0.68 ppm. The $HB(C_6F_5)_3^-$ anion is clearly identified by a broad doublet at 4.08 ppm in the $^1H$ NMR spectrum and a doublet at −25.2 ppm with $J_{B-H} = 70$ Hz in the $^{11}B$ NMR spectrum, which are in agreement with the formation of a hydroborate anion.[22] The $^{19}F$ NMR data closely match those of $[Bu_4N][HB(C_6F_5)_3]$,[22] indicating that the $[HB(C_6F_5)_3]^-$ anion is only weakly ion-paired to the aluminum cation in solution. The preparative-scale reaction of **6** allowed its isolation as a colorless solid in good yield (55%). Similarly to **4**, compound **6** slowly decomposes in halogenated solvents, but in this case the neutral adduct $(3,5\text{-}Me_2\text{-}C_3H_2N_2)B(C_6F_5)_3$ (**6a**) was isolated; its X-ray structure is reported in Figure 3. A possible mechanism for the formation of **6a** may involve the transfer of hydride from $HB(C_6F_5)^-$ to the coordinated ligand that is reminiscent of that proposed for the $B(C_6F_5)_3$-catalyzed hydroalumination of $Ph_2CO$ and PhCHO.[23]

The $\beta$-H abstraction with the concomitant alkene elimination is not very common in the reaction with $B(C_6F_5)_3$,[23,24] while it is generally observed when alkyl metal complexes with $\beta$-hydrogen are reacted with $[Ph_3C][B(C_6F_5)_4]$.[25] As a matter of fact, treatment of **3** with 1 equiv of $[Ph_3C][B(C_6F_5)_4]$ in $C_6D_6$ affords the $[(bpzmp)AliBu]^+[B(C_6F_5)_4]^-$ salt (**7**) in quantitative yield (Scheme 4) along with isobutene. **7** is less soluble than **6** in benzene and partially precipitates. The only difference between the $^1H$ NMR spectrum of **7** and **6** is the high-field shift for the resonance of the methyls at the 5 position of the pyrazolyl rings that is ascribed to the less coordinative character of the $[B(C_6F_5)_4]^-$ anion.[26] On the contrary, the reaction between **3** and $[HNMe_2Ph][B(C_6F_5)_4]$ in $C_6D_6$ proceeds by clean Al−R bond protonolysis to afford **7** and isobutane (Scheme 4). The formed $PhMe_2N$ appears not to be coordinated to the cationic aluminum center, on the basis of the chemical shift values.[27]

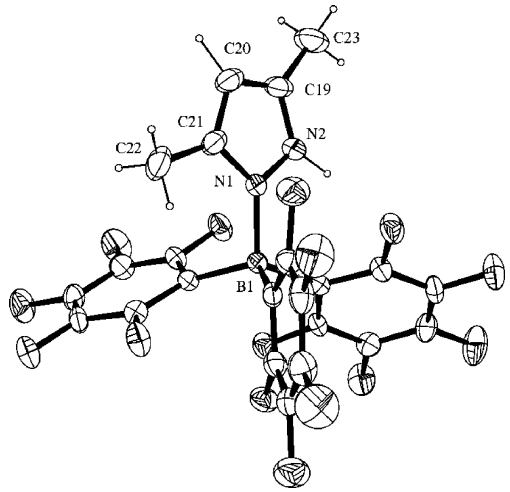


**Figure 3.** ORTEP view of **6a**. Thermal ellipsoids at the 30% probability level; only some of the atom labels are shown for clarity. Selected bond distances (Å): B1−N1 1.602(5), N1−N2 1.359(3), N1−C21 1.352(4), N2−C19 1.336(4).

**Table 2. Ring-Opening Polymerization of $\epsilon$-Caprolactone Initiated by [(*bpzmp*)AlMe][MeB($C_6F_5$)$_4$] (4)**

| entry[a] | [$\epsilon$-CL] (M) | [Al] (M) | [$\epsilon$-CL]/[Al] | conv (%) | yield[b] (g) |
|---|---|---|---|---|---|
| 1 | 1 | 0.02 | 50 | 99 | 0.25 |
| 2 | 1 | 0.01 | 100 | 99 | 0.50 |
| 3 | 1 | 0.006 | 150 | 98 | 0.74 |

[a] Reaction conditions: $4.5 \times 10^{-5}$ mol of **4**, toluene as solvent, 50 °C, 2 h. [b] *n*-Heptane-insoluble part.

No $^{27}Al$ NMR signals are observed for cationic species **4**−**6**; similar difficulties were already encountered in the literature. $^{27}Al$ NMR is not a useful probe for the structures of cationic aluminum species.[28]

**4. Ring-Opening Polymerization of $\epsilon$-Caprolactone Promoted by 4.** Ring-opening polymerization (ROP) of $\epsilon$-caprolactone ($\epsilon$-CL) catalyzed by complexes **1**−**6** is investigated. In general, polymerizations are carried out in toluene solution at 50 °C with a prescribed equivalent ratio of catalyst and monomer. The cationic methyl complex **4** is the only one found active in ROP of $\epsilon$-CL, the results being reported in Table 2.

The polymerization activity of **4** is comparable to that of neutral aluminum diamide[29] or ketiminate[30] complexes, although it is lower than those observed for early transition metal alkoxides.[31] The numerical molecular weights obtained from $^1H$ NMR analysis ($M_{n,NMR}$) of the polymers increase with the [M]/[Al] ratio in the feed of polymerization runs, but they are higher than theoretical ones ($M_{n,th}$) in the case of living

(20) Chen, E. Y. X.; Marks, T. J. *Chem. Rev.* **2000**, *100*, 1391.
(21) Horton, A. D.; de With, J.; Van der Linder, A. J.; Van de Weg, H. *Organometallics* **1996**, *15*, 2672.
(22) Blackwell, J. M.; Morrison, D. J.; Piers, W. E. *Tetrahedron* **2002**, *58*, 8247.
(23) Dagorne, S.; Janowska, I.; Welter, R.; Zakrzewski, J.; Jaouen, G. *Organometallics* **2004**, *23*, 4706.
(24) Walzer, D. A.; Woodman, T. J.; Schormann, M.; Hughes, D. L.; Bochmann, M. *Organometallics* **2003**, *22*, 797.
(25) (a) Korolev, A. V.; Ihara, E.; Guzei, I. A.; Young, V. G.; Jordan, R. F. *J. Am. Chem. Soc.* **2001**, *123*, 8291. (b) Jerkunica, J. M.; Taylor, T. G. *J. Am. Chem. Soc.* **1971**, *93*, 6278. (c) Hannon, J. S.; Taylor, T. G. *J. Org. Chem.* **1981**, *46*, 3645. For examples of $\beta$-H abstraction by $Ph_3C^+$ from transition metal alkyls see: (a) Beck, W.; Sunkel, K. *Chem. Rev.* **1988**, *88*, 1405. (b) Cheng, T.-Y.; Bullock, R. M. *Organometallics* **2002**, *21*, 2325.
(26) The ion-pairing interactions are not significant enough to perturb the $^{19}F$ spectrum of the $[B(C_6F_5)_4]^-$ anion.
(27) NMR data for free $NMe_2Ph$ in C6D6 are as follows: $\delta$ 7.24 (1H p-Ph), 6.80 (2H m-Ph), 6.62 (2H o-Ph), 2.50 (6H Me).
(28) (a) See ref 25a. (b) Masuda, J. D.; Walsh, D. M.; Wei, P.; Stephan, D. W. *Organometallics* **2004**, *23*, 1819.
(29) (a) Chakraborty, D.; Chen, E. Y. *Organometallics* **2002**, *21*, 1438. (b) Lewinski, J.; Horeglad, P.; Dranka, M.; Justyniak, I. *Inorg. Chem.* **2004**, *43*, 5789.
(30) Yu, R. C.; Hung, C. H.; Huang, J. H.; Lee, H. Y.; Chen, J. T. *Inorg. Chem.* **2002**, *41*, 6450.
(31) (a) McLain, S.; Drysdale, N. E. *Polym. Prepr.* **1992**, *33*, 174. (b) Evans, W. J.; Katsumata, H. *Macromolecules* **1994**, *27*, 2330.

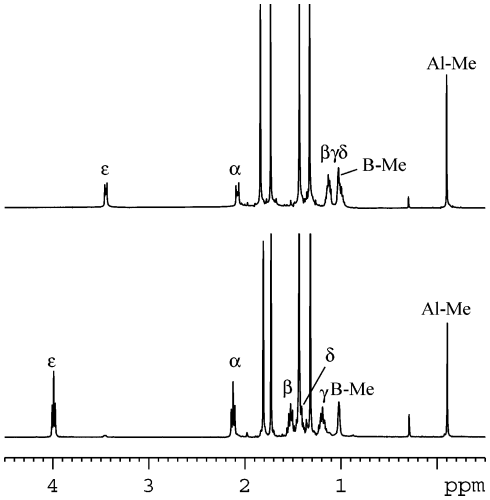


**Figure 4.** $^1$H NMR spectrum for the reaction of **4** and $\epsilon$-CL in a 1:1 ratio soon after the mixing of the reactants (top) and after 20 h at 50 °C (bottom) in $C_6D_6$. See the structure drawing in Scheme 5 for peak assignments of the labels $\alpha-\epsilon$.

**Scheme 5**

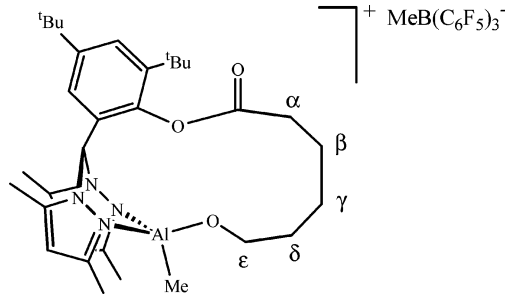


polymerization, indicating that only a part of the aluminum catalyst is active (about 30 mol %). To better understand the catalytic behavior of **4** in ROP polymerization of $\epsilon$-CL, the reaction between **4** and $\epsilon$-CL in a 1:1 molar ratio is monitored by $^1$H NMR spectroscopy. At room temperature only labile coordination of $\epsilon$-CL to the cationic electrophilic aluminum center is observed.[32] Upon heating the NMR tube at 50 °C, the slow reaction of $\epsilon$-CL occurs (8 mol % of conversion in 2 h, the complete conversion being reached in 24 h). The ring-opening product of $\epsilon$-CL is identified as a tetrahedral cationic alkoxide aluminum compound, [(*bpzphe*)AlMe]$^+$[MeB($C_6F_5$)$_4$]$^-$ (*bpzphe* = 2,4-di-*tert*-butyl-6-(bis(3,5-dimethylpyrazol-1-yl)-methyl)phenyl 6-hydroxyhexanoate) (**8**) (Scheme 5), whose molecular structure is defined by means of $^1$H NMR, 1D NOE, $^{13}$C NMR, COSY, and gHMQC experiments.

By analysis of NMR data it results that, in the ROP of $\epsilon$-CL promoted by **4**, the monomer insertion occurs into the Al−O bond of the *bpzmp* fragment and it does not involve the methyl group bonded at the aluminum center (Figure 4); a similar insertion of $\epsilon$-CL into the Al−heteroatom bond rather than into Al−Me was already observed[29] and is coherent with the generally accepted mechanism for ROP of $\epsilon$-CL promoted by metal alkoxides.[33] Complex **8** readily reacts with $\epsilon$-CL: $^1$H NMR monitoring of the reaction between **8** and 1 equiv of $\epsilon$-CL in $C_6D_6$ at 50 °C indicates a complete conversion of $\epsilon$-CL in 1 h. The NMR spectrum also suggests that the second insertion of $\epsilon$-CL occurs into the Al−O bond of the *bpzphe* fragment. The plot of the concentration of $\epsilon$-CL versus time follows a single-exponential decay, indicating a first-order dependence on monomer concentration for the second insertion of $\epsilon$-CL.

We can reasonably assume that in the ROP of $\epsilon$-CL promoted by **4** the polymerization starts with the insertion of $\epsilon$-CL into the Al−O bond of the *bpzmp* fragment to form the intermediate **8**, which leads to growth of the polymer chain through continuous insertions of the monomer in the Al−alkoxide bond.

## Conclusions

A series of neutral and cationic aluminum complexes **1**−**7** have been synthesized and characterized by X-ray diffraction analysis and VT NMR spectroscopy. The neutral dialkyl complexes **1**−**3** consist of a racemic mixture in which each stereoisomer adopts a tetrahedral structure. The *bpzmp* ligand is $\kappa^2$-coordinated to the metal via the phenoxy group and the imino nitrogen of one of the pyrazolyl rings. To the best of our knowledge this kind of coordination was never observed before. The solid-state structure is not retained in solution, and fluxional exchange between coordinated and noncoordinated pyrazolyl rings of the *bpzmp* ligand is observed. The dependence of the enthalpy of activation ($\Delta H^{\#}$) on the steric hindrance at the Al center suggests that the racemization process occurs through a displacement mechanism ($S_N2$) in which the pyrazolyl ring that is out of the coordination sphere displaces the pyrazolyl ring coordinated at the Al in a one-step reaction.

Reaction of neutral aluminum complexes **1**−**3** with the alkyl-abstracting agent (such as $B(C_6F_5)_3$ or $[Ph_3C][B(C_6F_5)_4]$) produces the expected cationic aluminum derivatives **4**−**6** as borate salts in which the *bpzmp* fragment is $\kappa^3$ coordinated to the aluminum center: the pendant pyrazolyl ring in the neutral precursor becomes a strong ligand, occupying the fourth coordination position in the cation, thereby stabilizing the electropositive aluminum center. The ionizing process for **3** depends on the character of acid employed: with a Lewis acid the reaction occurs by net $\beta$-H abstraction from the isobutyl group, forming isobutene along with the cationic complex, whereas with a Brönsted acid the reaction occurs by protonolysis of the butyl group with the concomitant formation of isobutane. In halogenated solvents, cations **4** and **6** slowly decompose, forming the salt **4a** and the neutral adduct **6a**, respectively. Efforts to understand the possible mechanisms for these decompositions are currently in progress.

Finally, complex **4** was active in ring-opening polymerization of $\epsilon$-caprolactone ($\epsilon$-CL), producing high-molecular-weight polymers. The $^1$H NMR monitoring of the reaction of **4** with $\epsilon$-CL in 1:1 molar ratio showed that the initiation of polymerization involves the slow monomer insertion into the Al−O bond of the *bpzmp* fragment, forming the intermediate (**8**), which in turn leads to the growth of the polymer chain through continuous insertion of the monomer in the Al−alkoxide bond.

## Experimental Section

**General Procedures.** All experiments were performed under nitrogen atmosphere using standard Schlenk-type techniques or an MBraun glovebox. Toluene and hexane were distilled from sodium/benzophenone. $C_6D_6$ and $C_7D_8$ were degassed under $N_2$ flow and stored over activated molecular sieves (4 Å) in a glovebox prior to use. NMR spectra were recorded on a Bruker AM300 and a Bruker

(32) The FT-IR spectrum of a 1:1 mixture of **4** and $\epsilon$-CL in $CH_2Cl_2$ shows two bands at 1729 and 1640 cm$^{-1}$ attributed to stretching of the carbonyl group in free $\epsilon$-CL and in the $\epsilon$-CL-**4** adduct, respectively (Lewinski, J.; Horeglad, P.; Tratkiewicz, E.; Grzenda, W.; Lipkowski, J.; Kolodziejczyk, E. *Macromol. Rapid Commun.* **2004**, *25*, 1939).

(33) Ropson, N.; Dubois, P.; Jerome, R.; Teyssie, P. *Macromolecules* **1995**, *28*, 7589.

AVANCE 400 operating at 300 and 400 MHz for $^1$H, respectively. The $^1$H and $^{13}$C chemical shifts are referenced to $SiMe_4$ using the residual protio impurities of the deuterated solvents as external reference. $^{27}$Al chemical shifts are reported versus Al(acac)$_3$, and $^{11}$B and $^{19}$F chemical shifts are reported versus $BF_3(OEt_2)$ and $CFCl_3$, respectively. Elemental analyses were performed with a Perkin-Elmer 240-C. Infrared spectra were recorded on a FT-IR Bruker Vector 22. $AlMe_3$, $AlEt_3$, and Al(*i*Bu)$_3$ (Aldrich) were checked for purity by $^1$H NMR and used as received. $B(C_6F_5)_3$, $[Ph_3C][B(C_6F_5)_4]$, and $[HNMe_2Ph][B(C_6F_5)_4]$ were purchased from Boulder Scientific and used as received. *Bpzmp*-H ligand was synthesized according to the literature procedure.[34] $\epsilon$-Caprolactone (Aldrich) was degassed and dried over $CaH_2$ overnight and then freshly vacuum distilled before use.

**Synthesis of (*bpzmp*)AlMe$_2$ (1).** A solution of $AlMe_3$ (1.72 mmol) in hexane (2.52 mL, 0.682 M) was added to a solution of *bpzmp*-H (0.520 g, 1.72 mmol) in hexane (50 mL, 0.0344 M) at room temperature. Evolution of methane was observed. The resulting pale yellow solution was stirred for 1 h. All volatiles were removed in vacuo, and the residue was extracted with toluene (40 mL). Filtration followed by concentrating the pale yellow filtrate and cooling the concentrated toluene solution at −10 °C afforded a white crystalline solid. Yield: 0.535 g (68%). Single crystals suitable for X-ray analysis were grown from saturated toluene solution at −20 °C. Anal. Calcd for $C_{27}H_{41}N_4OAl\cdot{}^1/_2C_7H_8$: C, 71.73; H, 8.88; N, 10.97. Found: C, 72.08; H, 8.94; N, 10.82. Spectroscopic data for (*bpzmp*)AlMe$_2$ (**1**): $^1$H NMR (400 MHz, toluene-$d_8$, 25 °C): $\delta$ −0.54 (bs, 6H, Al-*CH*$_3$), 1.32 (s, 9H, 5-*t*Bu-Ph), 1.60 (s, 9H, 3-*t*Bu-Ph), 1.81 (s, 6H, 3-C*H*$_3$-Pz), 2.05 (s, 6H, 5-C*H*$_3$-Pz), 5.46 (s, 2H, Pz-*H*), 6.81 (d, 1H, $J$ = 2.4 Hz, 6-*H*-Ar), 7.06 (s, 1H, −C*H*−), 7.58 (d, 1H, $J$ = 2.4 Hz, 4-*H*-Ar). $^{13}$C{$^1$H} NMR (100 MHz, $C_6D_6$, 25 °C): $\delta$ −7.42 (br), 12.25, 14.18, 30.71, 32.29, 34.60, 36.03, 77.52, 108.76, 121.77, 126.50, 127.40, 139.71, 140.67, 158.39. $^{27}$Al NMR (104.23 MHz, toluene-$d_8$, 100 °C): $\delta$ 145.7($W_{1/2}$ = 2684 Hz).

**Synthesis of (*bpzmp*)AlEt$_2$ (2).** A solution of $AlEt_3$ (1.22 mmol) in hexane (5.00 mL, 0.244 M) was added to a solution of *bpzmp*-H (0.500 g, 1.22 mmol) in hexane (50 mL, 0.0244 M) at room temperature. Evolution of ethane was observed. The resulting pale yellow solution was stirred for 1 h. The hexane solution was concentrated and cooled at −10 °C, affording 0.324 g of a crystalline white solid (54%). Single crystals suitable for X-ray analysis were grown by recrystallization from hexane at −20 °C. Anal. Calcd for $C_{29}H_{45}N_4OAl$: C, 70.70; H, 9.21; N, 11.37. Found: C, 70.88; H, 9.30; N, 11.25. Spectroscopic data for (*bpzmp*)AlEt$_2$ (**2**): $^1$H NMR (400 MHz, toluene-$d_8$, 25 °C): $\delta$ −0.10 (bs, 2H, Al-*CH*$_2$CH$_3$), 0.27 (bs, 2H, Al-*CH*$_2$CH$_3$), 1.23 (bs, 6H, Al-CH$_2$*CH*$_3$), 1.32 (s, 9H, 5-*t*Bu-Ph), 1.66 (s, 9H, 3-*t*Bu-Ph), 1.77 (bs, 6H, 3-C*H*$_3$-Pz), 2.10 (s, 6H, 5-C*H*$_3$-Pz), 5.46 (bs, 2H, Pz-*H*), 6.73 (s, 1H, −C*H*−), 6.97 (d, 1H, $J$ = 2.4 Hz, 6-*H*-Ar), 7.53 (d, 1H, $J$ = 2.4 Hz, 4-*H*-Ar). Selected $^{13}$C{$^1$H} NMR data (100 MHz, $C_6D_6$, 25 °C): $\delta$ 0.21 (vbr), 2.86 (vbr) 9.92, 12.20, 13.96, 30.61, 32.24, 34.56, 36.09, 77.56, 108.66 (br), 121.65, 126.55, 127.44, 139.66, 140.59, 158.94.

**Synthesis of (*bpzmp*)Al*i*Bu$_2$ (3).** A solution of Al*i*Bu$_3$ (1.22 mmol) in hexane (5.00 mL, 0.244 M) was added to a solution of *bpzmp*-H (0.500 g, 1.22 mmol) in hexane (50 mL, 0.0244 M) at room temperature. Evolution of isobutane was observed. The resulting pale yellow solution was stirred for 1 h and concentrated. The resulting pale yellow solution was cooled at −10 °C, affording 0.467 g of a crystalline white solid (70%). Single crystals suitable for X-ray analysis were grown by recrystallization from hexane at −20 °C. Anal. Calcd for $C_{33}H_{53}N_4OAl$: C, 72.22; H, 9.73; N, 10.21. Found: C, 72.43; H, 9.81; N, 10.13. Spectroscopic data for (*bpzmp*)Al*i*Bu$_2$ (**3**): $^1$H NMR (400 MHz, toluene-$d_8$, 25 °C): $\delta$ 0.13 (q, 2H, $J$ = 6.7 Hz, Al-*CH*$_2$CH(CH$_3$)$_2$), 0.23 (m, 2H, Al-*CH*$_2$CH-(CH$_3$)$_2$), 0.86 (dd, 6H, $J_1$ = 6.7 Hz, $J_2$ = 3.8 Hz, Al-CH$_2$CH(*CH*$_3$)$_2$), 1.14 (dd, 2H, $J_1$ = 10.0 Hz, $J_2$ = 6.7 Hz, Al-CH$_2$CH(*CH*$_3$)$_2$), 1.30 (s, 9H, 5-*t*Bu-Ph), 1.57 (s, 3H, 3-C*H*$_3$-Pz), 1.60 (s, 9H, 3-*t*Bu-Ph), 1.73 (m, 1H, Al-CH$_2$C*H*(CH$_3$)$_2$), 1.98 (m, 1H, Al-CH$_2$C*H*(CH$_3$)$_2$), 1.84 (s, 3H, 3-C*H*$_3$-Pz), 2.08 (s, 3H, 5-C*H*$_3$-Pz), 2.18 (s, 3H, 5-C*H*$_3$-Pz), 5.41 (s, 1H, Pz-*H*), 5.61 (s, 1H, Pz-*H*), 6.78 (brs, 1H, 6-*H*-Ar), 7.05 (s, 1H, −C*H*−), 7.55 (d, 1H, $J$ = 2.6 Hz, 4-*H*-Ar). $^{13}$C{$^1$H} NMR (75 MHz, $C_6D_6$, 25 °C): $\delta$ 12.09, 12.15, 14.14, 14.29, 23.30 (br), 25.08 (br), 26.82, 26.98 28.64, 28.84, 28.95, 29.41, 31.08, 32.22, 34.57, 36.17, 77.27, 107.49, 108.57, 108.77, 122.52, 126.61, 127.45, 139.97, 140.63, 146.84, 147.67, 151.69, 159.34. $^{27}$Al NMR (104.23 MHz, toluene-$d_8$, 100 °C): $\delta$ 142.5($W_{1/2}$ = 4360 Hz).

**Synthesis of [(*bpzmp*)AlMe][MeB(C$_6$F$_5$)$_3$] (4).** In a 100 mL round-bottom flask, (*bpzmp*)AlMe$_2$ (**1**) (100 mg, 0.215 mmol) and $B(C_6F_5)_3$ (110 mg, 0.215 mmol) were added and dissolved in 20 mL of $CH_2Cl_2$. The resulting pale yellow solution was stirred for 30 min at room temperature and then evaporated to dryness to yield a pale yellow foam. Trituration with cold hexane provoked the precipitation of a colorless solid. The solvent was filtered off by cannula and the solid residue dried under vacuum to afford [(*bpzmp*)AlMe][MeB(C$_6$F$_5$)$_3$] (**4**) as a colorless solid (150 mg, 70%). Anal. Calcd for $C_{45}H_{41}AlBF_{15}N_4O$: C, 55,34; H, 4,23; N, 5,74. Found: C, 55.97; H, 4.86; N, 5.42 Spectroscopic data for [(*bpzmp*)-AlMe]$^+$: $^1$H NMR (400 MHz, $C_6D_6$, 25 °C): $\delta$ −0.12 (s, 3H, Al-C*H*$_3$), 1.30 (s, 9H, 5-*t*Bu-Ph), 1.43 (s, 9H, 3-*t*Bu-Ph), 1.69 (s, 6H, 3-C*H*$_3$-Pz), 1.77 (s, 6H, 5-C*H*$_3$-Pz), 5.04 (s, 2H, Pz-*H*), 6.69 (s, 1H, −C*H*−), 6.94 (d, 1H, $J$ = 2.2 Hz, 6-*H*-Ar), 7.56 (d, 1H, $J$ = 2.2 Hz, 4-*H*-Ar). Selected $^{13}$C{$^1$H} NMR data (100 MHz, $C_6D_6$, 25 °C): $\delta$ −14.1 (Al-*C*H$_3$), 10.6 (5-C*H*$_3$-Pz), 12.1 (3-C*H*$_3$-Pz), 29.9 (3-*t*Bu-Ph), 31.8 (5-*t*Bu-Ph), 72.7 (*C*H−), 109.4 (4-*C*-Pz), 125.1 (6-*C*-Ar), 129.1 (6-*C*-Ar). Spectroscopic data for [MeB(C$_6$F$_5$)$_3$]$^-$: $^1$H NMR (400 MHz, $C_6D_6$, 25 °C): $\delta$ 0.96 (BC*H*$_3$). $^{13}$C{$^1$H} NMR (100 MHz, $C_6D_6$, 25 °C): $\delta$ 11.8 (B*C*H$_3$). $^{19}$F NMR (376 MHz, $C_6D_6$, 25 °C): $\delta$ −132.5 (d, $^3J_{FF}$ = 19.4 Hz, 2F, *o*-C$_6$*F*$_5$), −164.9 (t, $^3J_{FF}$ = 19.4 Hz, 2F, *m*-C$_6$*F*$_5$), −167.6 (t, $^3J_{FF}$ = 19.4 Hz, 1F, *p*-C$_6$*F*$_5$).

**Generation of [(*bpzmp*)AlEt][EtB(C$_6$F$_5$)$_3$] (5).** In a glovebox, equimolar amounts of (*bpzmp*)AlEt$_2$ (**2**) (6 mg, 0.012 mmol) and $B(C_6F_5)_3$ (7 mg, 0.012 mmol) were added in a sample vial and dissolved in 0.7 mL of $C_6D_6$. The resulting pale yellow solution was transferred in a NMR tube (10 mm o.d.) and analyzed at 25 °C. Spectroscopic data for [(*bpzmp*)AlEt]$^+$: $^1$H NMR (400 MHz, $C_6D_6$, 25 °C): $\delta$ 0.47 (q, 2H, $J$ = 8.3 Hz, Al-*CH*$_2$CH$_3$), 1.31 (s, 9H, 5-*t*Bu-Ph), 1.36 (t, 3H, $J$ = 8.3 Hz, Al-CH$_2$*CH*$_3$), 1.43 (s, 9H, 3-$^t$Bu-Ph), 1.74 (s, 6H, 3-C*H*$_3$-Pz), 1.79 (s, 6H, 5-C*H*$_3$-Pz), 5.07 (s, 2H, Pz-*H*), 6.71 (s, 1H, −C*H*−), 6.96 (d, 1H, $J$ = 2.4 Hz, 6-*H*-Ar), 7.56 (d, 1H, $J$ = 2.4 Hz, 4-*H*-Ar). Selected $^{13}$C{$^1$H} NMR data (100 MHz, $C_6D_6$, 25 °C): $\delta$ −3.3 (Al-*C*H$_2$CH$_3$), 7.9 (Al-CH$_2$*C*H$_3$), 10.9 (5-*C*H$_3$-Pz), 12.2 (3-*C*H$_3$-Pz), 29.9 (3-*t*Bu-Ph), 31.8 (5-*t*Bu-Ph), 72.8 (−*C*H−), 109.5 (4-*C*-Pz), 125.0 (6-*C*-Ar), 129.1 (4-*C*-Ar). Spectroscopic data for [EtB(C$_6$F$_5$)$_3$]$^-$: $^1$H NMR (400 MHz, $C_6D_6$, 25 °C): $\delta$ 1.08 (t, 2H, $J$ = 7.3 Hz, BC*H*$_2$CH$_3$), 1.72 (bq, 3H BCH$_2$C*H*$_3$). $^{13}$C{$^1$H} NMR (100 MHz, $C_6D_6$, 25 °C): $\delta$ 13.2 (B*C*H$_2$CH$_3$), 15.4 (BCH$_2$*C*H$_3$). $^{19}$F NMR (376 MHz, $C_6D_6$, 25 °C): $\delta$ −131.9 (d, $^3J_{FF}$ = 22.2 Hz, 2F, *o*-C$_6$*F*$_5$), −165.0 (t, $^3J_{FF}$ = 22.2 Hz, 2F, *m*-C$_6$*F*$_5$), −167.6 (t, $^3J_{FF}$ = 22.2 Hz, 1F, *p*-C$_6$*F*$_5$).

**Synthesis of [(*bpzmp*)Al*i*Bu][HB(C$_6$F$_5$)$_3$] (6).** In a 100 mL round-bottom flask, (*bpzmp*)Al*i*Bu$_2$ (**3**) (130 mg, 0.237 mmol) and $B(C_6F_5)_3$ (121 mg, 0.237 mmol) were added and dissolved in 20 mL of $CH_2Cl_2$. The resulting pale yellow solution was stirred for 30 min at room temperature and then evaporated to dryness to yield a pale yellow foam. Trituration with cold hexane provoked the precipitation of a colorless solid. The solvent was filtered off by cannula and the solid residue dried under vacuum to afford [(*bpzmp*)Al*i*Bu][HB(C$_6$F$_5$)$_3$] (**6**) as a colorless solid (133 mg, 55%).

(34) (a) The, K. I.; Peterson, L. K. *Can. J. Chem.*, **1973**, *51*, 422. (c) Hammes, B. S.; Carrano, C. J. *Inorg. Chem.* **1999**, *38*, 3562.

**Table 3. Crystal, Collection, and Refinement Data for (*bpzmp*)AlMe$_2$ (1), (*bpzmp*)AlEt$_2$ (2), and (*bpzmp*)Al*i*Bu$_2$ (3)**

| | 1 | 2 | 3 |
|---|---|---|---|
| formula | $C_{27}H_{41}N_4OAl\cdot{}^1/_2C_7H_8$ | $C_{29}H_{45}N_4OAl$ | $C_{33}H_{53}N_4OAl$ |
| fw | 510.7 | 492.7 | 548.8 |
| $T$ (K) | 173 | 173 | 173 |
| cryst syst | triclinic | monoclinic | triclinic |
| space group | $P\bar{1}$ | $P2_1/c$ | $P\bar{1}$ |
| $a$ (Å) | 9.587(7) | 14.871(3) | 9.430(2) |
| $b$ (Å) | 11.231(6) | 12.175(3) | 9.479(2) |
| $c$ (Å) | 15.06(1) | 17.426(3) | 19.711(4) |
| α (deg) | 70.75(4) | | 100.72(2) |
| $\beta$ (deg) | 81.86(5) | 109.73(2) | 91.81(2) |
| $\gamma$ (deg) | 87.92(4) | | 104.60(2) |
| $V$ (Å$^3$) | 1515(2) | 2970(2) | 1669(1) |
| $Z$ | 2 | 4 | 2 |
| $D_c$ (g cm$^{-3}$) | 1.12 | 1.10 | 1.092 |
| $\mu$ (mm$^{-1}$) | 0.095 | 0.094 | 0.090 |
| $\theta$ max (deg) | 27.5 | 27.5 | 27.5 |
| no. of unique reflns | 6862 | 6701 | 7395 |
| no. of obs reflns [$I > 2\sigma(I)$] | 2726 | 3550 | 4907 |
| $R_1$ (obs) | 0.0846 | 0.0657 | 0.0562 |
| $wR_2$ (all data) | 0.2660 | 0.1834 | 0.1755 |
| no. of params | 388 | 325 | 382 |
| $\Delta\rho_{max}$; $\Delta\rho_{min}$ (e Å$^{-3}$) | 0.386; −0.571 | 0.513; −0.305 | 0.568; −0.363 |

Anal. Calcd for $C_{47}H_{45}AlBF_{15}N_4O$: C, 56,19; H, 4,51; N, 5,58. Found: C, 56.78; H, 4.98; N, 5.83. Spectroscopic data for [(*bpzmp*)-Al*i*Bu]$^+$: $^1$H NMR (400 MHz, $C_6D_6$, 25 °C): $\delta$ 0.68 (d, 2H, $J$ = 7.6 Hz, Al-C*H*$_2$CHMe$_2$), 1.23 (d, 6H, $J$ = 6.5, Hz, Al-CH$_2$CH*Me*$_2$), 1.29 (s, 9H, 5-*t*Bu-Ph), 1.42 (s, 9H, 3-*t*Bu-Ph), 1.80 (s, 6H, 3-C*H*$_3$-Pz), 1.91 (s, 6H, 5-C*H*$_3$-Pz), 2.28 (m, 1H, AlCH$_2$C*H*Me$_2$), 5.15 (s, 2H, Pz-*H*), 6.92 (s, 1H, −C*H*−), 7.10 (d, 1H, $J$ = 2.6 Hz, 6-*H*-Ar), 7.66 (d, 1H, $J$ = 2.6 Hz, 4-*H*-Ar). Selected $^{13}$C{$^1$H} NMR data (100 MHz, $C_6D_6$, 25 °C): $\delta$ 10.9 (5-*C*H$_3$-Pz), 12.8 (3-*C*H$_3$-Pz), 18.4 (Al-*C*H$_2$CHMe$_2$), 26.1 (AlCH$_2$*C*HMe$_2$), 28.6 (Al-CH$_2$-CH*Me*$_2$), 29.9 (3-*t*Bu-Ph), (31.7 5-*t*Bu-Ph), 72.6 (−*C*H−), 109.4 (4-*C*-Pz), 125.0 (6-*C*-Ar), 128.6 (4-*C*-Ar). Spectroscopic data for [HB(C$_6$F$_5$)$_3$]$^-$: $^1$H NMR (400 MHz, $C_6D_6$, 25 °C): $\delta$ 4.08 (vbr s, 1H, B*H*). $^{19}$F NMR (376 MHz, $C_6D_6$, 25 °C): $\delta$ −133.30 (d, $^3J_{FF}$ = 22.2 Hz, 2F, *o*-C$_6$*F*$_5$), −164.24 (t, $^3J_{FF}$ = 19.4 Hz, 2F, *m*-C$_6$*F*$_5$), −167.30 (t, $^3J_{FF}$ = 22.2 Hz, 1F, *p*-C$_6$*F*$_5$). $^{11}$B NMR (−25.19 MHz, $C_6D_6$, 25 °C): $\delta$ −25.2 ($J_{BH}$ = 70.2 Hz). Spectroscopic data for 2-methylprop-1-ene are as follows: $^1$H NMR (400 MHz, $C_6D_6$, 25 °C): $\delta$ 1.60 (t, 6H, $J$ = 1.2 Hz, *Me*$_2$C=CH$_2$), 4.85 (m, 6H, $J$ = 1.2 Hz, Me$_2$C=C*H*$_2$)

**Generation of [(*bpzmp*)Al*i*Bu][B(C$_6$F$_5$)$_4$] (7).** In a glovebox, equimolar amounts of (*bpzmp*)Al*i*Bu$_2$ (**3**) (6 mg, 0.011 mmol) and [Ph$_3$C][B(C$_6$F$_5$)$_4$] (10 mg, 0.011 mmol) or [PhNMe$_2$H][B(C$_6$F$_5$)$_4$] (9 mg, 0.011 mmol) were added in a sample vial and dissolved in 0.7 mL of $C_6D_6$. The resulting pale yellow solution was transferred in a NMR tube (10 mm o.d.) and analyzed at 25 °C. Spectroscopic data for [(*bpzmp*)Al*i*Bu][B(C$_6$F$_5$)$_4$]: $^1$H NMR (400 MHz, $C_6D_6$, 25 °C): $\delta$ 0.62 (d, 2H, $J$ = 7.6 Hz, Al-*C*H$_2$CHMe$_2$), 1.25 (d, 6H, $J$ = 6.5, Hz, Al-CH$_2$CH*Me*$_2$), 1.31 (s, 9H, 5-*t*Bu-Ph), 1.43 (s, 9H, 3-*t*Bu-Ph), 1.78 (s, 6H, 3-C*H*$_3$-Pz), 1.80 (s, 6H, 5-C*H*$_3$-Pz), 2.26 (m, 1H, AlCH$_2$C*H*Me$_2$) 5.09 (s, 2H, Pz-*H*), 6.65 (s, 1H, −C*H*−), 6.96 (d, 1H, $J$ = 2.4, Hz, 6-*H*-Ar), 7.79 (d, 1H, $J$ = 2.4 Hz, 4-*H*-Ar). $^{19}$F NMR (376 MHz, $C_6D_6$, 25 °C): $\delta$ −132.29 (d, $^3J_{FF}$ = 11.0 Hz, 2F, *o*-C$_6$*F*$_5$), −163.19 (t, $^3J_{FF}$ = 19.2 Hz, 2F, *m*-C$_6$*F*$_5$), −167.18 (t, $^3J_{FF}$ = 19.2 Hz, 1F, *p*-C$_6$*F*$_5$). Spectroscopic data for 2-methyl-1-propene: $^1$H NMR (400 MHz, $C_6D_6$, 25 °C): $\delta$ 1.60 (t, 6H, $J$ = 1.2 Hz, *Me*$_2$C=CH$_2$), 4.85 (m, 6H, $J$ = 1.2 Hz, Me$_2$C=C*H*$_2$). Spectroscopic data for 2-methylpropane: $^1$H NMR (400 MHz, $C_6D_6$, 25 °C): $\delta$ 0.86 (d, 1H, $J$ = 6.5 Hz, *Me*$_3$CH), 1.63 (m, 9H, $J$ = 6.5 Hz, Me$_3$C*H*).

**Generation of [(*bpzphe*)AlMe][MeB(C$_6$F$_5$)$_3$] (8) on a NMR Scale.** In a glovebox, $\epsilon$-CL (2.3 $\mu$L, 20 $\mu$mol) dissolved in benzene-$d_6$ (0.3 mL) was added to a solution of [(*bpzmp*)AlMe][MeB(C$_6$F$_5$)$_3$] (**4**) (20 $\mu$mol) in benzene-$d_6$ (0.4 mL) in a NMR tube. The resulting solution was heated at 50 °C for 24 h and then analyzed by NMR spectroscopy. Spectroscopic data for [(*bpzphe*)AlMe][MeB(C$_6$F$_5$)$_3$]: $^1$H NMR (400 MHz, $C_6D_6$, 25 °C): $\delta$ −0.12 (s, 3H, Al-*CH*$_3$), 0.99 (s, 3H, B-*CH*$_3$) 1.18 (m, 2H, O-CH$_2$CH$_2$*CH*$_2$CH$_2$CH$_2$-CO), 1.31 (s, 9H, 5-*t*Bu-Ph), 1.40 (m, 2H, O-CH$_2$*CH*$_2$CH$_2$CH$_2$CH$_2$-CO), 1.43 (s, 9H, 3-*t*Bu-Ph), 1.52 (m, 2H, O-CH$_2$CH$_2$CH$_2$*CH*$_2$CH$_2$-CO), 1.70 (s, 6H, 3-C*H*$_3$--Pz), 1.79 (s, 6H, 5-C*H*$_3$-Pz), 2.12 (t, 2H, $J$ = 7.5 Hz, O-CH$_2$CH$_2$CH$_2$CH$_2$*CH*$_2$-CO), 3.99 (t, 2H, $J$ = 6.7 Hz, O-*CH*$_2$CH$_2$CH$_2$CH$_2$CH$_2$-CO), 5.04 (s, 2H, Pz-*H*), 6.71 (s, 1H, −C*H*−), 6.97 (d, 1H, $J$ = 2.4 Hz, 6-*H*-Ar), 7.56 (d, 1H, $J$ = 2.4 Hz, 4-*H*-Ar). Selected $^{13}$C{$^1$H} NMR data (100 MHz, $C_6D_6$, 25 °C): $\delta$ −14.2 (Al-*C*H$_3$), 10.5 (5-C*H*$_3$-Pz), 12.1 (3-C*H*$_3$-Pz), 25.1, (O-CH$_2$CH$_2$CH$_2$*C*H$_2$CH$_2$-CO) 25.9 (O-CH$_2$CH$_2$*C*H$_2$CH$_2$CH$_2$-CO), 29.7 (3-*t*Bu-Ph), 31.6 (5-*t*Bu-Ph), 34.5 (O-CH$_2$CH$_2$CH$_2$CH$_2$*C*H$_2$-CO), 64.2 (O-*C*H$_2$CH$_2$CH$_2$CH$_2$CH$_2$-CO), 72.5 (*C*H−), 109.1 (4-*C*-Pz), 124.9 (6-*C*-Ar), 128.8 (6-*C*-Ar). $^{19}$F NMR (376 MHz, $C_6D_6$, 25 °C): $\delta$ −132.5 (d, $^3J_{FF}$ = 25.8 Hz, 2F, *o*-C$_6$*F*$_5$), −164.9 (t, $^3J_{FF}$ = 21.2 Hz, 2F, *m*-C$_6$*F*$_5$), −167.6 (t, $^3J_{FF}$ = 21.2 Hz, 1F, *p*-C$_6$*F*$_5$).

**$\epsilon$-Caprolactone Polymerization Initiated by [(*bpzmp*)AlMe]-[MeB(C$_6$F$_5$)$_4$] (4).** A general procedure for $\epsilon$-caprolactone polymerization catalyzed by aluminum complexes is herein described. A 21 mg sample of **1** (45 $\mu$mol) and 23 mg of B(C$_6$F$_5$)$_3$ (45 $\mu$mol) were dissolved in the appropriate amount of toluene (2 mL for run 1). After equilibration of the solution at 50 °C the reaction was started by injection of the appropriate amount of $\epsilon$-caprolactone (0.25 mL for run 1 [M]/[Al] = 50). The solution was stirred for 2 h to produce a gel-like polymer. Methylene chloride was added to dissolve the polymer gel, and the resulting solution was poured into an excess of *n*-heptane to precipitate poly-$\epsilon$-caprolactone. Crude products were recrystallized from THF/hexane and dried in vacuo to constant weight.

**Crystal Structure Determinations.** Crystal data and collection details are reported in Table 3 for **1**, **2**, and **3** and in the Supporting Information for **4a** and **6a**. The most relevant bond distances and angles are reported in the figure captions. Single crystals used for X-ray analysis were placed in glue on the top of a glass pin and quickly transferred to the cold stream of the diffractometer. Data collections were performed under $N_2$ flux at −100 °C on a Bruker-Nonius KappaCCD single-crystal diffractometer with monochromated Mo Kα ($\lambda$ = 0.71073 Å) radiation. Data were collected and integrated using the Bruker Nonius COLLECT software package,[35] and semiempirical absorption corrections were applied (multiscan

(35) *COLLECT*, Data collection software; Nonius BV: Delft, The Netherlands, 1999.

SADABS[36]). All structures were solved by direct methods (Sir97[37]) and refined by the full matrix least-squares method on $F^2$ against all independent measured reflections (SHELXL-97[38]). All non-hydrogen atoms were refined with anisotropic displacement parameters. H atoms were placed in idealized positions and refined by a riding model with thermal parameters $U_{iso}$ set to the $U_{eq}$ of the carrier atom.

Statistical disorder was found for one *tert*-butyl group of **1**, for one ethyl group of **2**, and for one isobutyl group of **3**. The two split positions in **1** and **2** were refined with 0.5 occupation factor, while in **3** the occupation factor level was refined (0.688). A disordered solvate molecule of toluene with half occupancy is present in **1** located near an inversion center so that some constraints were included in order to obtain regular geometric parameters of the ring.

(36) *SADABS*, area detector scaling and absorbption correction; Bruker AXS, 2002.

(37) Altomare, A.; Burla, M. C.; Camalli, M.; Cascarano, G. L.; Giacovazzo, C.; Guagliardi, A.; Moliterni, A. G. G.; Polidori, G.; Spagna, R. *J. Appl. Crystallogr.* **1999**, *32*, 115−119.

(38) Sheldrick, G. M. *SHELXL-97*, Programs for Crystal Structure Analysis (Release 97-2); Institüt für Anorganische Chemie der Universität: Tammanstrasse 4, D-3400 Göttingen, Germany, 1998.

All crystallographic data have been deposited with the Cambridge Crystallographic Data Center (CCDC). Deposition numbers are CCDC 266621−266623 for **1**−**3** and 286538−286539 for **4a** and **6a**. These data can be obtained free of charge at www.ccdc.cam.ac.uk/conts/retrieving.html or from the Cambridge Crystallographic Data Centre, 12 Union Road, Cambridge CB2 1EZ, UK [fax: (internat.) +44-1223/336-033; e-mail: deposit@ccdc.cam.ac.uk].

**Acknowledgment.** We are grateful to Prof. P. Longo and Prof. A. Grassi for helpful discussions. This work was supported by Italian Ministry of University. Thanks are also due to Centro Regionale di Competenza−NTAP of Regione Campania (Italy) and CIMCF of Università di Napoli "Federico II" for X-ray equipment.

**Supporting Information Available:** ORTEP view for **2** and **3**, $^1$H NMR spectra of **1**−**8**, 2D NMR experiments, determination of the kinetic parameters for the racemization processes for **1**−**3**; full crystallographic data given as a CIF file. This material is available free of charge via the Internet at http://pubs.acs.org.

OM050902E